THE JOURNAL OF BIOLOGICAL CHEMISTRY VOL. 287, NO. 35, pp. 29312–29323, August 24, 2012

The Wnt Receptor Ryk Plays a Role in Mammalian Planar Cell Polarity Signaling*

Received for publication, March 15, 2012, and in revised form, June 27, 2012 Published, JBC Papers in Press, July 6, 2012, DOI 10.1074/jbc.M112.362681

Maria L. Macheda[‡§], Willy W. Sun[¶], Kumudhini Kugathasan[§], Benjamin M. Hogan[§‖], Neil I. Bower[‖], Michael M. Halford[‡§], You Fang Zhang[‡§], Bonnie E. Jacques[¶], Graham J. Lieschke[§1], Alain Dabdoub[¶], and Steven A. Stacker[‡§2]**

*From the [‡]Tumour Angiogenesis Program, Peter MacCallum Cancer Centre, East Melbourne, Victoria 3002, Australia, the [§]Ludwig Institute for Cancer Research, Parkville, Victoria 3050, Australia, the [¶]Department of Surgery/Division of Otolaryngology, University of California at San Diego School of Medicine, La Jolla, California 92093, the [‖]Institute for Molecular Biosciences, University of Queensland, St Lucia, Queensland 4072, Australia, and the **Sir Peter MacCallum Department of Oncology, University of Melbourne, Victoria 3010, Australia*

Background: Ryk acts as a Wnt receptor in several processes, including mouse neuronal development.
Results: Ryk interacts with Wnt11 in zebrafish convergent extension and with Vangl2 in mouse cochlear development and neural tube closure.
Conclusion: Ryk is required for Wnt/planar cell polarity signaling during mammalian development and signals via Vangl2 and RhoA.
Significance: This study extends our knowledge of signaling downstream of Ryk.

Wnts are essential for a wide range of developmental processes, including cell growth, division, and differentiation. Some of these processes signal via the planar cell polarity (PCP) pathway, which is a β-catenin-independent Wnt signaling pathway. Previous studies have shown that Ryk, a member of the receptor tyrosine kinase family, can bind to Wnts. Ryk is required for normal axon guidance and neuronal differentiation during development. Here, we demonstrate that mammalian Ryk interacts with the Wnt/PCP pathway. *In vitro* analysis showed that the Wnt inhibitory factor domain of Ryk was necessary for Wnt binding. Detailed analysis of two vertebrate model organisms showed Ryk phenotypes consistent with PCP signaling. In zebrafish, gene knockdown using morpholinos revealed a genetic interaction between Ryk and Wnt11 during the PCP pathway-regulated process of embryo convergent extension. Ryk-deficient mouse embryos displayed disrupted polarity of stereociliary hair cells in the cochlea, a characteristic of disturbed PCP signaling. This PCP defect was also observed in mouse embryos that were double heterozygotes for *Ryk* and *Looptail* (containing a mutation in the core Wnt/PCP pathway gene *Vangl2*) but not in either of the single heterozygotes, suggesting a genetic interaction between Ryk and Vangl2. Co-immunoprecipitation studies demonstrated that RYK and VANGL2 proteins form a complex, whereas RYK also activated RhoA, a downstream effector of PCP signaling. Overall, our data suggest an important role for Ryk in Wnt/planar cell polarity signaling during vertebrate development via the Vangl2 signaling pathway, as demonstrated in the mouse cochlea.

Wnt signaling is necessary for a wide range of developmental processes, including cell growth, division, and differentiation. Signaling via the β-catenin-independent Wnt/planar cell polarity (PCP)[3] pathway is required for several processes in early development (1). PCP signaling regulates cell polarization, the coordinated orientation of cellular structures within the plane of an epithelium along an axis perpendicular to the apical-basal axis, and directed cellular movements.

During gastrulation, cells become polarized and converge mediolaterally by intercalation, leading to extension of the anterior-posterior axis, a process referred to as convergent extension (CE) (2). Studies of *Xenopus laevis* and zebrafish gastrulation and CE showed that Wnt11 and the intracellular Wnt pathway protein Dishevelled (Dvl) are important regulators of gastrulation via the PCP pathway (3–5).

Mouse knock-outs for several PCP pathway genes have shown similar phenotypes. One of the most extensively studied is the spontaneous mouse mutant *Looptail*. Mice heterozygous for this mutation in the *Vangl2* gene, $Vangl2^{Lp/+}$, have a curly tail that can be seen in embryos as well as adults, whereas homozygous mice ($Vangl2^{Lp/Lp}$) die at birth, have severe neural tube defects, and disrupted polarity of hair cell stereociliary bundles in the cochlea (6–8). In addition, mice that are double heterozygotes for two Wnt/PCP pathway genes, such as $Vangl2^{Lp/+}$ with *Wnt5a*, *Dvl3*, or the Scribble1 mutant

* This work was supported in part by a program grant (to S. A. S.) from the National Health and Medical Research Council of Australia and Grant R01DC011104 (to A. D.) from the National Institutes of Health.
[1] Present address: Australian Regenerative Medicine Institute, Monash University, Clayton, Victoria 3800, Australia.
[2] Supported by a Senior Research Fellowship from the National Health and Medical Research Council of Australia and a Pfizer Australia Fellowship. To whom correspondence should be addressed: Peter MacCallum Cancer Centre, Locked Bag 1, A'Beckett St., Melbourne, Victoria 8006, Australia. Tel.: 61-3-9656-5263; Fax: 61-3-9656-1411; E-mail: steven.stacker@petermac.org.

[3] The abbreviations used are: PCP, planar cell polarity; CE, convergent extension; Dvl, Dishevelled; Fzd, Frizzled; WIF, Wnt inhibitory factor; MEF, mouse embryonic fibroblast; E, embryonic day; ECD, extracellular domain; WD, WIF domain; MO, morpholino; GST-RBD, GST-Rhotekin binding domain; hpf, hours post-fertilization; P, postnatal day; OHC, outer hair cell; IHC, inner hair cell; TCF, T cell factor.

Crc, display the same neural tube and cochlear defects as *Vangl2*$^{Lp/Lp}$ mice, indicating a genetic interaction (8–10).

Ryk is a cell surface protein with homology to the receptor tyrosine kinase family (11, 12). Although kinase-inactive, Ryk acts as a Wnt receptor in both invertebrates and vertebrates (13, 14). Ryk-deficient mice die on the day of birth; they have craniofacial and skeletal defects, axon guidance defects, and fewer forebrain neurons (15–17). *In vitro* studies have shown that Ryk directly interacts with Wnts, the Wnt receptor Frizzled (Fzd) 8, and with Dvl (16, 18–20). The Ryk extracellular region contains a Wnt inhibitory factor (WIF) domain that is believed to be required for Wnt binding (16, 21). Ryk has been shown to function as a Wnt receptor in processes including rodent axon repulsion, axon extension and neuronal differentiation, zebrafish lateral mesoderm cell migration, and *X. laevis* convergent extension (14, 16, 17, 19, 22–24).

Here, we show that Wnts bind to the Ryk WIF domain and that Ryk interacts with the Wnt/PCP pathway during embryonic development. Disrupted cochlear hair cell orientation, a characteristic PCP defect, was observed in Ryk-deficient mouse embryos and in *Ryk* and *Vangl2*^{Lp} double-heterozygous embryos. In addition, we show that RYK protein interacts with the PCP pathway protein VANGL2 *in vitro* and that RYK activates RhoA, a downstream effector of Wnt-Vangl2 signaling. These findings demonstrate that Ryk is an important mediator of Wnt/PCP signaling in mammals during development.

EXPERIMENTAL PROCEDURES

Cell Lines—HEK293T and CHO-K1 cells and mouse embryonic fibroblasts (MEFs) were maintained in DMEM (Invitrogen) supplemented with 10% FBS and were incubated at 37 °C in 10% CO_2.

MEFs were generated using E13.5 mouse embryos from *Ryk*$^{+/-}$ × *Ryk*$^{+/-}$ matings. Postmortem embryos had their heads and abdominal organs removed, were placed in a syringe with 1 ml of 0.1% trypsin/versene, passed through an 18-gauge needle several times, and then digested at 37 °C for 30 min. Digested embryos were triturated and incubated at 37 °C for 15 min. The resulting cells (called passage 0) were plated in 10-cm tissue culture plates in DMEM + 10% FBS. MEFs were used up to passage 5 for TCF-luciferase reporter assays.

Mouse and Zebrafish Maintenance—Mice and zebrafish were maintained in accordance with the Australian National Health and Medical Research Council "Australian Code of Practice for the Care and Use of Animals for Scientific Purposes 2004" and in accordance with National Institutes of Health and University of California at San Diego guidelines for the care and use of laboratory animals. All experimental procedures on live animals were approved by the Ludwig Institute for Cancer Research Animal Ethics Committee or the Peter MacCallum Cancer Centre Animal Experimentation Ethics Committee. The generation and genotyping of Ryk-deficient mice have been described previously (15). *Vangl2*$^{Lp/+}$ mice were originally purchased from The Jackson Laboratory (LPT/LeJ). *Ryk*$^{+/-}$;*Vangl2*$^{Lp/+}$ double heterozygotes were obtained by mating a *Ryk*$^{+/-}$ mouse on a 129T2/Sv genetic background with a *Vangl2*$^{Lp/+}$ mouse.

Vangl2 genotyping was performed using the following primers: Vangl2-R 5′-AAGAGGAAGTAGGACTGGCAG-3′, V2wt^{LNA} 5′-CAAACAGTGGACCTTGGTGaG-3′, and V2Lp^{LNA} 5′-CAAACAGTGGACCTTGGTGaA-3′, where the lowercase letter indicates an LNA nucleotide. The PCR utilized one pair of primers, V2wt^{LNA} or V2Lp^{LNA} forward primer and Vangl2-R reverse primer, with Platinum *Pfx* polymerase (Invitrogen) and the following cycling conditions: one cycle at 94 °C for 3 min and then 30 cycles at 94 °C for 15 s, 63 °C for 15 s, 68 °C for 30 s, and finally one cycle at 68 °C for 5 min.

DNA Constructs—The mouse Ryk constructs used were as follows: mature mouse Ryk extracellular domain (ECD; residues 34–211 of GenBank™ accession number NP_038677.3); Ryk extracellular domain with a deleted WIF domain (residues 34–47 fused to 179–211); Ryk WIF domain alone (WD; residues 48–177); Ryk extracellular domain lacking the region amino-terminal of the WD (DN; residues 48–211); and Ryk extracellular domain lacking the region carboxyl-terminal of the WD (DC; residues 34–179). These Ryk constructs were subcloned by PCR into pApex-3.Fc.FLAG, between an IL-3 signal peptide and the human IgG_1 Fc domain, to create fusion proteins with a carboxyl-terminal FLAG epitope tag. In addition, we used mature full-length mouse Ryk (from residue 34) with an IL-3 signal peptide at the amino terminus and a FLAG epitope tag inserted at the carboxyl terminus between residues 585 and 586, producing pcDNA3.mRykFCT.

The human RYK constructs used were as follows: mature full-length RYK (from residue 47 of GenBank™ accession number NP_002949.2) with an IL-3 signal peptide at the amino terminus and a FLAG epitope tag inserted at the carboxyl terminus between residues 598 and 599, producing pcDNA3.hRYKFCT; or full-length RYK with an IL-3 signal peptide and a 2× Myc epitope tag at the amino terminus, producing pcDNA3.Myc2.hRYK; a RYK PDZ-binding motif mutant similar to pcDNA3.Myc2.hRYK, with deletion of the final four RYK residues, called pcDNA3.Myc2.hRYKΔPDZBM; the entire human RYK ECD (residues 47–227) or the RYK WD alone (residues 60–195), with an IL-3 signal peptide at the amino terminus, subcloned by PCR into pApex-3.Fc.FLAG, or into pcDNA3 with a FLAG tag at the carboxyl terminus.

The human WIF-1 cDNA was purchased from OriGene Technologies. Full-length WIF-1 was subcloned by PCR into pApex-3.Fc.FLAG; the WIF-1.RYKWD construct was subcloned by PCR into pApex-3.Fc.FLAG and includes human WIF-1 with the endogenous WD (residues 32–181 of GenBank™ accession number NP_009122.2) replaced with the human RYK WD (residues 60–198). Mouse Wnt3a and Wnt11 cDNAs were a kind gift from Dr. Andrew McMahon (Harvard University). Mature Wnt1, Wnt3a, Wnt5a, and Wnt11 were subcloned into pcDNA3, with a 5× Myc epitope tag at the carboxyl terminus, to create pcDNA3.Wnt1/Wnt3a/Wnt5a/Wnt11.Myc5. The human VANGL2 cDNA was from Dr. Randall Moon (purchased from Addgene, plasmid 16992). Full-length VANGL2 was subcloned by PCR into pcDNA3, with a 2× HA epitope tag at the amino terminus, to create pcDNA3.HA2.hVANGL2.

Production and Purification of RYK.Fc, WIF-1.Fc, and WIF-1.RYKWD.Fc Proteins—RYK.Fc/CHO, WIF-1.Fc/CHO, and WIF-1.RYKWD.Fc/CHO stable cell line generation and WIF-1.Fc and WIF-1.RYKWD.Fc protein production were performed as described previously for RYKWD.Fc (23). RYK.Fc/CHO cells were seeded into pleated surface roller bottles (BD Biosciences) using DMEM + 10% FBS + 100 μg/ml hygromycin B. Conditioned medium was collected from roller bottles after 5 days. Secreted protein was purified using anti-FLAG M2 affinity gel (Sigma) as described previously (25).

Immunoprecipitation and Western Blots—HEK293T cells were transiently transfected using FuGENE 6 (Invitrogen) and lysed 24 h post-transfection in lysis buffer (150 mM NaCl, 50 mM Tris, pH 7.5, 1% Triton X-100, 1× Complete (Roche Diagnostics), 1 mM sodium orthovanadate). Proteins were immunoprecipitated with M2 affinity gel (Sigma) for FLAG-tagged proteins, 9E10-conjugated Sepharose for Myc-tagged proteins, and 12CA5-conjugated Sepharose for HA-tagged proteins. Immunoprecipitates were washed three times with PBS + 0.1% Triton X-100 and eluted in sample buffer. Western blotting was performed as described previously (16). Primary antibodies used were anti-FLAG M2-HRP (Sigma) and anti-Myc 9E10-HRP and anti-HA high affinity (Roche Diagnostics).

Luciferase Assays— 40,000 HEK293T cells were seeded into 24-well plates and transfected the next day with 100 ng of superTOP-FLASH or superFOP-FLASH vectors (a kind gift from Dr. Randall Moon, University of Washington), 100 ng of RYK or WIF-1 construct vector, and 1 ng of *Renilla* luciferase vector pRL-CMV (Promega), using FuGENE 6. Cells were treated 24 h post-transfection with serum-free medium containing diluent or purified mouse Wnt3a (R&D Systems), lysed 24 h after treatment, and analyzed using the Dual-Luciferase reporter assay (Promega). The ratio of firefly to *Renilla* luciferase was used for statistical analysis, with a one-way analysis of variance and Tukey's multiple comparison post hoc test.

MEFs were transfected using Nucleofector (Lonza) program A-23. 1×10^6 cells were nucleofected using the MEF1 Nucleofector Solution (Lonza) and 1 μg of TOP-FLASH or FOP-FLASH vectors. 5.5×10^4 cells were seeded into 24-well plates, serum-starved 24 h post-nucleofection in DMEM + 0.2% BSA, and then treated 24 h after serum starvation with serum-free medium containing diluent or 20 ng/ml purified Wnt3a. Cells were lysed 24 h after treatment, and a luciferase assay was performed using the Luciferase Assay System (Promega).

Zebrafish Morpholino Experiments—Morpholinos (MOs) were synthesized by Gene Tools, LLC. MO injection of one-cell embryos was performed using a constant volume of MOs (1.77 nl). The dose of MO injected was optimized for each MO so as to not produce nonspecific effects. *Ryk* mRNA was targeted with two MOs, each injected at 5 ng/embryo. Ryk MO-1 overlaps the ATG site, 5′-GTGGGCTGGATGTTTCTGCCAGCG-3′; Ryk MO-2 is targeted to the 5′ UTR, 5′-GATGAGGTTCCGTGGCGCTGGTCGA-3′. The Wnt11 MO is from Ref. 26 and was injected at 2.5 ng/embryo. *VANGL2* mRNA was transcribed from the human VANGL2 cDNA in plasmid pCS2P$^+$ (Addgene plasmid 16992) using SP6 RNA polymerase and the MessageAmp RNA amplification kit (Ambion) and was injected at 200 pg/embryo. Uninjected embryos were used as controls. Live embryos were photographed at 54 h post-fertilization (hpf) in benzocaine to determine length and then were fixed in 4% paraformaldehyde/PBS for later scoring of eye phenotype. Embryos were imaged with a Nikon stereo microscope and a Nikon DMX1200C camera. Embryo length was measured in the photographs; eye phenotype was scored on a four-point scale, where 0 = wild-type eye distance and 3 = eyes fused. Multiple groups were compared using a one-way analysis of variance with Tukey's multiple comparison post hoc test.

Mouse Cochlea Analysis—Mouse embryos were collected at E18.5, and their heads were removed and stored overnight in 4% paraformaldehyde/PBS and then in PBS for at least 24 h. Cochleae were dissected out and processed as whole mounts, and stereociliary bundles were labeled with either Alexa 488-conjugated phalloidin (Invitrogen) or a biotin-conjugated *Griffonia simplicifolia* lectin (Vector Laboratories). Stereociliary bundle orientation data were collected from a minimum of three embryos and 30 cells per hair cell row per embryo, as described previously (27). Multiple groups were compared using a one-way analysis of variance with Tukey's multiple comparison post hoc test; two groups were compared using unpaired *t* tests. Histograms represent the number of hair cells in 5° intervals (*e.g.* 11–15° stereociliary bundle orientation).

β-Galactosidase Staining, Immunohistochemistry, and Immunofluorescence—Immunohistochemistry was performed on cochleae as described previously (28). Briefly, fixed E18.5 cochleae were dissected and reacted for β-gal activity with X-Gal (Sigma) overnight at 37 °C. Cochleae were then sectioned in a cryostat at 12 μm and immunostained with anti-myosin 6 antibody (1:1000; Proteus BioSciences). For Ryk immunofluorescence, whole mount cochleae from postnatal day (P) 0 wild-type CD-1 ICR mice were stained with anti-Ryk antibody (1:250; a kind gift from Dr. Yimin Zou, (19)), followed by Alexa-conjugated secondary antibody (Invitrogen) and phalloidin.

Active RhoA Pulldowns—GST-Rhotekin binding domain (GST-RBD), which binds only to active RhoA (RhoA-GTP), was prepared by lysing Rosetta2 cells containing pGEX-RBD plasmid (a kind gift from Dr. Raymond Habas, Temple University) with BugBuster Master Mix (Novagen) supplemented with 1× Complete (EDTA-free; Roche Diagnostics), 10 mM DTT, and 10 mM $MgCl_2$. GST-RBD bacterial lysate was incubated with glutathione-Sepharose 4 Fast Flow (GE Healthcare) and washed three times with lysis buffer (see below). CHO-K1 cells were transfected in 10-cm plates with cDNAs using Lipofectamine 2000 (Invitrogen) and lysed 24 h post-transfection in 1 ml of lysis buffer: 200 mM NaCl, 50 mM Tris, pH 7.2, 1% Nonidet P-40, 10% glycerol, 1× Complete (EDTA-free), and 1× PhosStop (Roche Diagnostics). CHO-K1 cells transfected with both RYK siRNA and Wnt3a were transfected first with RYK siRNA (human RYK siGENOME SMARTpool, gene ID 6259; Thermo Scientific) using DharmaFECT 1 transfection reagent and then after 24 h with Wnt3a.Myc5 cDNA using Lipofectamine 2000, and cells were lysed 24 h after cDNA transfection.

Pulldowns were performed using cell lysate and GST-RBD-Sepharose for 30 min, washed three times using lysis buffer, and

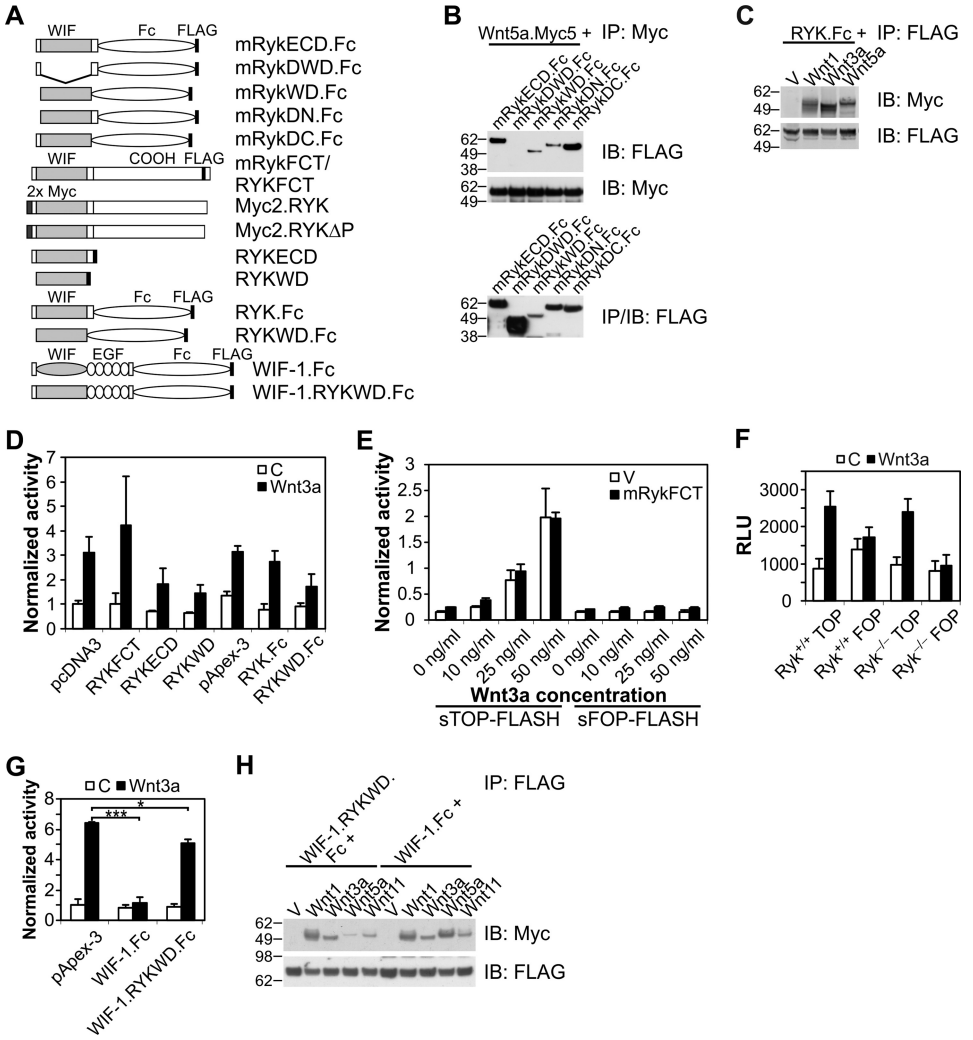

FIGURE 1. **Interaction of Ryk with Wnts and Wnt/β-catenin signaling assays.** *A*, Ryk and WIF-1 constructs used in co-immunoprecipitation experiments and TCF-luciferase reporter assays. *B*, immunoprecipitation of 400 μg of lysate from HEK293T cells transfected with mouse Ryk.Fc constructs and Wnt5a.Myc5. *IP*, immunoprecipitation; *IB*, immunoblot. *C*, co-immunoprecipitation of 200 μg of lysate from HEK293T cells transfected with empty vector (*V*), Wnt1.Myc5, Wnt3a.Myc5, or Wnt5a.Myc5, and 500 ng of purified RYK.Fc protein. *D*, TCF-luciferase reporter assays of HEK293T cells transfected with RYK constructs, superTOP-FLASH and *Renilla*, and treated with diluent (*C*) or 25 ng/ml purified Wnt3a for 24 h. Data are normalized to empty vector-transfected cells. The *graph* shows the mean ± S.D. of two to four independent experiments of triplicate determinations. No statistically significant differences were observed. *E*, TCF-luciferase reporter assay of HEK293T cells transfected with superTOP-FLASH and superFOP-FLASH reporters and treated with purified Wnt3a at various concentrations for 24 h. The *graph* shows the mean ± S.D. of one experiment of triplicate determinations. *F*, TCF-luciferase reporter assays of MEFs from $Ryk^{+/+}$ or $Ryk^{-/-}$ embryos transfected with TOP-FLASH (containing three TCF sites in promoter) or FOP-FLASH (containing mutated TCF sites in promoter) and treated with 20 ng/ml purified Wnt3a for 24 h. The *graph* shows the mean ± S.E. of three independent experiments of triplicate determinations. No statistically significant differences were observed. *RLU*, relative luciferase units. *G*, TCF-luciferase reporter assays of HEK293T cells transfected with WIF-1.Fc constructs, superTOP-FLASH and *Renilla*, and treated with 25 ng/ml purified Wnt3a for 24 h. Data are normalized to empty vector-transfected cells. The *graph* shows the mean ± S.D. of two independent experiments of triplicate determinations. *, $p < 0.05$; ***, $p < 0.001$. *H*, co-immunoprecipitation of 200 μg of lysate from HEK293T cells transfected with empty vector (*V*), Wnt1.Myc5, Wnt3a.Myc5, Wnt5a.Myc5, or Wnt11.Myc5 and 1 μg of purified WIF-1.RYKWD.Fc or WIF-1.Fc protein.

eluted in sample buffer. Western blotting of the pulldowns and cell lysates was performed with anti-RhoA mouse monoclonal antibody 26C4 (Santa Cruz Biotechnology). Band intensity was quantified using Odyssey software (LI-COR Biosciences), and the intensity of each active RhoA band (from pulldown) was normalized to total RhoA band intensity (from cell lysate). Two groups were compared used an unpaired *t* test.

RESULTS

Interaction of the Ryk WIF Domain with Wnt5a—To determine the regions of Ryk required for Wnt binding, several mouse Ryk extracellular domain (ECD) mutants were constructed as fusion proteins with the human IgG_1 Fc domain, to create soluble Ryk-derived proteins (Fig. 1*A*). After co-expression of these FLAG-tagged Ryk ECD proteins with Myc-tagged mouse Wnt5a in HEK293T cells, lysates were immunoprecipitated and analyzed by Western blotting. Full-length Ryk ECD (mRykECD.Fc) co-immunoprecipitated with Wnt5a; however, a Ryk ECD construct with the WIF domain (WD) deleted (mRykDWD.Fc) did not immunoprecipitate with Wnt5a (Fig. 1*B*). Furthermore, Ryk constructs containing the WD alone (mRykWD.Fc) or the WD with either the amino- or carboxyl-terminal region of the ECD (mRykDC.Fc or mRykDN.Fc, respectively) interacted strongly with Wnt5a (Fig. 1*B*). Re-probing of blots with anti-Myc antibody and anti-FLAG immunoprecipitation/probing demonstrated equivalent levels

of Wnt5a and expression of Ryk fusion proteins, respectively, in all immunoprecipitations. These results demonstrated that Wnt5a interaction with Ryk is dependent on the Ryk WIF domain.

Wnt5a.Myc5 from cell lysate may be interacting with co-expressed Ryk constructs in the cytoplasm. To control for this possibility, immunoprecipitation experiments were performed using purified human RYK extracellular domain construct (RYK.Fc) protein (Fig. 1*A*). Wnt1, Wnt3a, and Wnt5a were all able to co-immunoprecipitate with RYK.Fc (Fig. 1*C*), suggesting that the interaction of Ryk with Wnts is independent of co-expression.

Ryk Fails to Modulate Wnt/β-Catenin Signaling in Vitro—Modulation of Wnt/β-catenin signaling can be studied using *in vitro* TCF-luciferase reporter assays, where β-catenin translocation to the nucleus is quantified by luciferase activity. A previous study using TCF-luciferase reporter assays demonstrated that Ryk activates the Wnt/β-catenin pathway in conjunction with Wnt3a treatment (18). We attempted to confirm and extend these results using full-length human RYK, RYK.Fc, or other constructs of RYK ECD (Fig. 1*A*). Transcriptional reporter assays performed using HEK293T cells transfected with superTOP-FLASH (a TCF-luciferase reporter) showed no difference in luciferase activity in control-treated cells transfected with RYK constructs compared with empty vector-transfected cells (Fig. 1*D*). Increased luciferase activity was observed after Wnt3a treatment, which was not further increased in cells transfected with either full-length human RYK (RYKFCT), RYK ECD, or RYK WD constructs (Fig. 1*D*). Titration of Wnt3a showed no difference in luciferase activity between cells overexpressing full-length mouse Ryk (mRykFCT) and empty vector-transfected cells at any of the Wnt3a concentrations tested (Fig. 1*E*). In addition, TCF reporter assays performed using $Ryk^{+/+}$ or $Ryk^{-/-}$ mouse embryonic fibroblasts (MEFs) showed no difference in Wnt3a-stimulated luciferase activity (Fig. 1*F*). These results suggest that Ryk overexpression is unable to stimulate Wnt/β-catenin signaling in these cells.

Transfection of the Wnt/β-catenin pathway inhibitor WIF-1 (WIF-1.Fc construct) into HEK293T cells completely inhibited Wnt3a-stimulated luciferase activity (Fig. 1*G*). To see if the RYK WD has an inhibitory function similar to the WIF-1 WD, a WIF-1/RYK WD chimeric construct, WIF-1.RYKWD.Fc, was made (Fig. 1*A*) and used in TCF reporter assays. The construct significantly inhibited Wnt3a stimulation, although this inhibition was not as strong as that observed with WIF-1.Fc (Fig. 1*G*). These results show that Ryk overexpression is unable to stimulate Wnt/β-catenin signaling and is only weakly able to inhibit Wnt3a-stimulated signaling in HEK293T cells.

To show that WIF-1.RYKWD.Fc is able to interact with Wnts, purified WIF-1.Fc or WIF-1.RYKWD.Fc protein was co-immunoprecipitated with lysates from HEK293T cells transfected with Myc-tagged Wnts. Both proteins were able to interact with Wnt1, Wnt3a, Wnt5a, and Wnt11 (Fig. 1*H*). Thus WIF-1.RYKWD.Fc interacts with the same Wnts as WIF-1.Fc, although the endogenous WIF-1 WIF domain is more effective at inhibiting Wnt/β-catenin signaling than the RYK WIF domain.

Zebrafish Convergent Extension Provides Evidence for Ryk Participation in Wnt/PCP Signaling—We used zebrafish to explore the role of Ryk in vertebrate development, in an attempt to identify phenotypes associated with β-catenin-independent Wnt signaling. During embryonic development, Wnt signaling drives CE movements to determine embryo length. As well as extending the axial length, extension of the anterior axis splits an initial singular eye field to produce two separate eyes (29). Zebrafish CE is driven by Wnt11, with *wnt11*/*silverblick* mutants displaying a shortened axis and severely reduced interocular distances or cyclopia (5). To determine the effect of Ryk gene knockdown in zebrafish, two MOs were designed, one spanning the Ryk start ATG site (Ryk MO-1) and the other upstream and nonoverlapping in the 5′ UTR (Ryk MO-2). Injection of 5 ng of Ryk MO-1 but not Ryk MO-2 alone at the one-cell stage resulted in a significant reduction in embryo length at 54 hpf (Fig. 2, *A*, *B,* and *D*).

As Ryk is a Wnt receptor, a synergistic effect may be expected after co-injection of Ryk MOs with MOs directed to Wnts. Wnt11 MO injection in zebrafish embryos has been shown to affect body length and reduce eye distance (26, 30). Consequently, zebrafish embryos were injected with Wnt11 MO alone or in combination with each Ryk MO. Wnt11 MO-injected embryos at 54 hpf had no significant reduction in body length (Fig. 2*D*) but displayed a mild eye phenotype (Fig. 2, *E*–*G*). Wnt11 MO in combination with either Ryk MO showed a further reduction in body length compared with single MO-injected embryos (Fig. 2, *C* and *D*). Injection of Wnt11 MO + Ryk MO-1 did not increase the percentage of embryos displaying an eye phenotype from that seen with Wnt11 MO alone but led to a small nonstatistically significant increase in phenotypic severity. However, Wnt11 MO co-injected with Ryk MO-2 led to a statistically significant increase in both the percentage and severity of eye phenotypes from that seen with Wnt11 MO alone ($p < 0.0001$, χ^2 analysis; Fig. 2*G*), supporting the genetic interaction observed in body axis length. The data suggest that Ryk acts synergistically with Wnt11 in zebrafish development to alter Wnt signaling-dependent CE. Furthermore, these effects are in processes mediated by Wnt/PCP signaling.

Ryk-deficient Mice Display an Inner Ear Phenotype Characteristic of Disrupted PCP Signaling—Our previous experiments suggested that Ryk is involved in Wnt/PCP signaling. We therefore examined Ryk-deficient mice for evidence of phenotypes generated by disruption of this pathway. One well characterized mouse defect associated with PCP pathway signaling is the disrupted orientation of the stereociliary bundles of cochlear hair cells. In wild-type mice, stereociliary bundles of all hair cells are oriented toward the lateral edge of the cochlear duct (Fig. 3*A*), whereas mice with mutations in the PCP genes *Celsr1*, *Vangl2,* and *Scrib1* have stereociliary bundles that are severely misoriented, with some bundles rotated almost 180° (8, 31). To determine whether $Ryk^{-/-}$ mice had disrupted stereociliary bundle orientation, cochleae from E18.5 mice (on a 129T2/Sv genetic background) were examined. $Ryk^{-/-}$ mice had misoriented bundles in the third row of outer hair cells (OHC) (Fig. 3*B*). These differences were statistically significant ($p = 0.005$; Fig. 3*C*). Histograms of stereociliary bundle orientation further illustrate the disrupted orientation of the third row of OHCs in

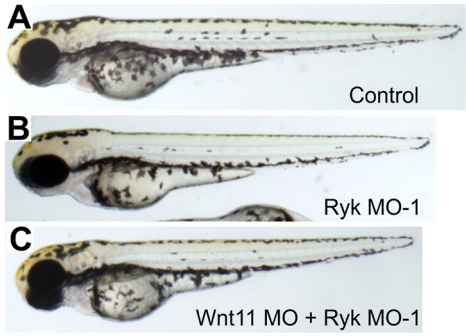

D

	Control (n)	Ryk MO-1 (n)	Ryk MO-2 (n)	Wnt11 MO (n)	Wnt11 MO+ Ryk MO-1 (n)	Wnt11 MO+ Ryk MO-2 (n)
Mean body length (mm)	3.18 (120)	3.08 (40)	3.12 (40)	3.13 (120)	2.96 (80)	2.97 (80)
SD (mm)	0.11	0.08	0.10	0.12	0.15	0.17
ANOVA vs. C (*P*)		<0.001	ns	ns	<0.001	<0.001
ANOVA vs. Wnt11 MO (*P*)		ns	ns		<0.001	<0.001

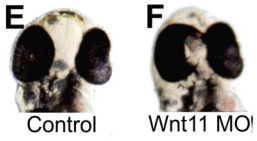

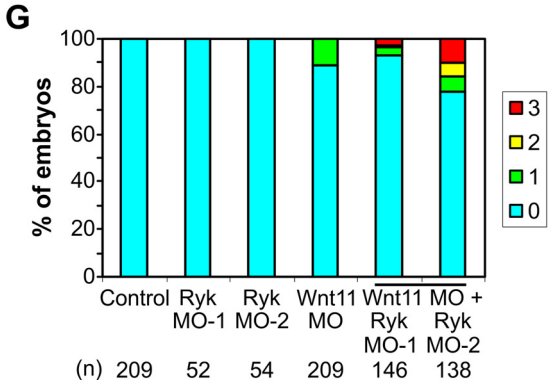

FIGURE 2. **Effects of Ryk and Wnt11 knockdown in zebrafish embryos at 54 hpf.** *A*, lateral view of an uninjected control embryo. *B*, example of an embryo injected with Ryk MO-1, which had reduced body length. *C*, example of an embryo injected with Wnt11 MO + Ryk MO-1, showing significantly reduced body length. *D*, quantitation of body length in embryos injected with Ryk MO-1, Ryk MO-2, and Wnt11 MO. (*n*), number of embryos analyzed in each treatment; *SD*, standard deviation of body length; *C*, control embryos. *E*, frontal view of a control embryo, showing normal eye spacing. *F*, frontal view of an embryo injected with Wnt11 MO, showing eyes touching. *G*, quantitation of eye phenotype in zebrafish embryos injected with Ryk MOs and/or Wnt11 MO. Eye phenotype was defined as follows: *0* = wild-type; *1* = eyes close together or just touching; *2* = eyes partly fused; *3* = eyes fused. (*n*), number of embryos analyzed in each treatment. *ANOVA*, analysis of variance.

$Ryk^{-/-}$ mice (OHC3; Fig. 3*D*). In contrast, $Ryk^{+/-}$ mice had normal bundle orientation compared with wild-type littermates in all hair cells (see Fig. 6). This phenotype in Ryk-deficient embryos suggests that Ryk plays a role in regulating PCP pathway signaling in the mouse cochlea.

Ryk Expression in Mouse Cochlea—To determine whether Ryk is expressed in the mouse cochlea during development, E18.5 embryo and P0 mouse heads were examined. $Ryk^{-/-}$ E18.5 embryo heads were stained to detect β-gal, which is expressed from the interrupted *Ryk* allele and so can be used as a proxy for *Ryk* mRNA expression (15). Strong *Ryk* mRNA expression was observed in pillar cells, located between the inner hair cells (IHCs) and OHCs, and in all three rows of OHCs, and it was confirmed by co-expression of *Ryk* mRNA with myosin 6, a marker of sensory hair cells (Fig. 4*A*). Immunofluorescence staining of P0 cochlea showed Ryk protein expression in pillar cells and all OHC rows, but not in IHCs (Fig. 4*B*). Therefore, Ryk mRNA and protein are expressed in mouse cochlea during development.

Interaction between Ryk and the Wnt/PCP Pathway in Mouse Development—To investigate whether Ryk interacts with Vangl2, a core member of the PCP signaling pathway, we analyzed the phenotype of embryos derived from $Ryk^{+/-}$ and $Vangl2^{Lp/+}$ mice. $Ryk^{+/-}$ mice and $Vangl2^{Lp/+}$ mice have none of the major developmental phenotypes that are associated with the $Ryk^{-/-}$ and $Vangl2^{Lp/Lp}$ mouse embryos. Analysis of 22 double-heterozygous mouse embryos ($Ryk^{+/-}$;$Vangl2^{Lp/+}$) showed that 9% had severe defects in neural tube development (Fig. 5*A*). No littermates of other genotypes showed these defects; all embryos had a genetic background of one part 129T2/Sv to one part LeJ. The embryos displayed defective neural tube development resulting in the brain and spinal cord remaining open, called craniorachischisis. This pathology is characteristic of the neural tube defects seen in *Looptail* mice, $Vangl2^{Lp/Lp}$ (6, 7). In addition, 13% of $Ryk^{-/-}$ mouse embryos (2 out of 15) displayed exencephaly, a less severe defect where the neural tube remains open only at the head (Fig. 5*B*). This phenotype is background-dependent, as it was observed in mice with a 129T2/Sv genetic background but not in C57BL/6 × 129T2/Sv mixed background mice.

Analysis of the cochleae of E18.5 mice showed that $Ryk^{+/-}$ single heterozygotes had no defects in stereociliary bundle orientation, whereas $Vangl2^{Lp/+}$ single heterozygotes showed a mild rotation of stereociliary bundles in the third row of OHCs (Fig. 6*A*), as observed previously (9). However, double heterozygotes had significantly more severely misoriented third row OHC bundles compared with single heterozygote littermates (Fig. 6, *A* and *B*), as was also clear in stereociliary bundle orientation histograms (Fig. 6*C*). These studies demonstrate that Ryk interacts with the PCP pathway to control developmental processes in the nervous system and cochlea.

RYK Interacts with and Activates Wnt/PCP Pathway Proteins—To determine whether the RYK and VANGL2 proteins are able to interact, HA-tagged human VANGL2 and Myc-tagged full-length human RYK constructs (Fig. 1*A*) were used. The extreme carboxyl terminus of RYK contains a PDZ-binding motif that is involved in protein-protein interactions (15). Therefore, we made a human RYK construct with the final four carboxyl-terminal residues deleted (Myc2.RYKΔPDZBM). Transfection of HEK293T cells with full-length RYK or VANGL2 followed by immunoprecipitation showed that RYK was able to co-immunoprecipitate with VANGL2 and vice versa (Fig. 7*A*). Deletion of the RYK PDZ-binding motif greatly reduced the ability of RYK to interact with VANGL2 (Fig. 7*A*). These results suggest that RYK protein forms a complex with

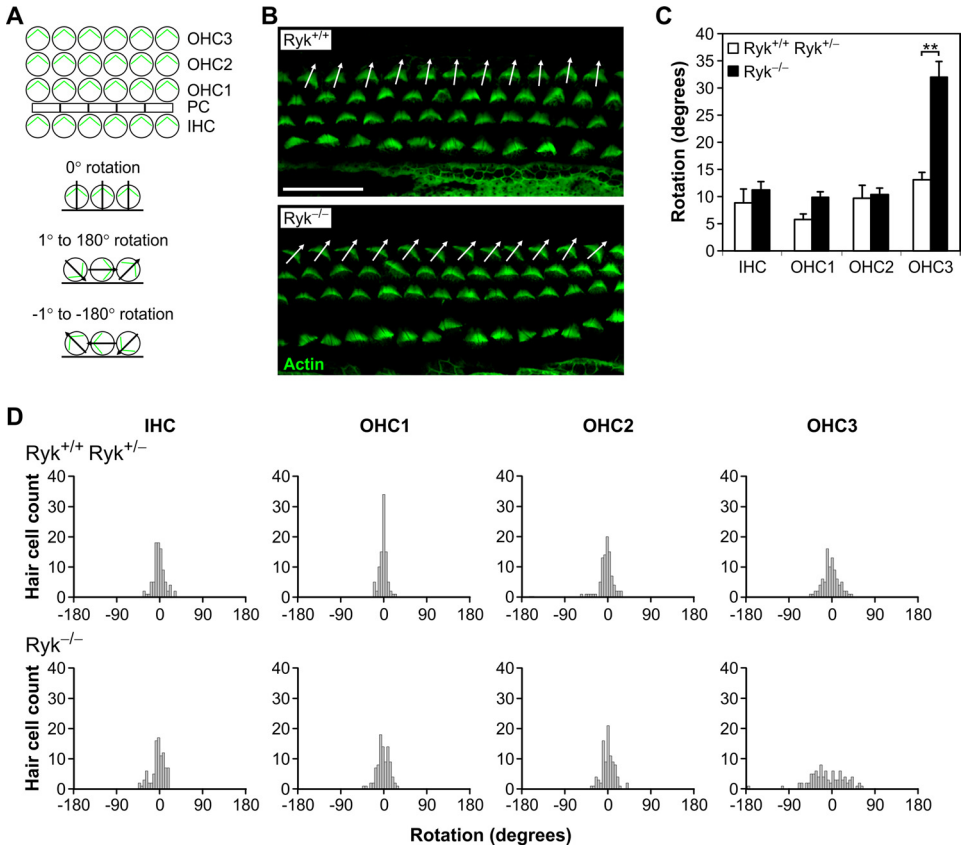

FIGURE 3. **Ryk-deficient mice demonstrate a role for Ryk in the PCP pathway.** *A*, schematic representations of stereociliary bundle orientation in cochlear hair cells of wild-type mice and showing the 0° base line of cell rotation, rotation to the left of center (negative degrees), and rotation to the right of center (positive degrees). Abbreviations used are as follows: *IHC*, inner hair cell; *OHC*, outer hair cell; *PC*, pillar cell. *B*, orientation of stereociliary bundles in E18.5 $Ryk^{+/+}$ and $Ryk^{-/-}$ mouse embryos, as observed at the mid-point of the sensory epithelia by staining with phalloidin (to detect actin). *Arrows* show the orientation of the third row outer hair cells (OHC3). Many cells in $Ryk^{-/-}$ embryos have a misoriented bundle orientation. *Scale bar*, 20 μm. *C*, analysis of the orientation of hair cell stereociliary bundles. Results represent the mean ± S.E. for three embryos. **, $p < 0.01$. *D*, distribution histograms of stereociliary bundle orientation in E18.5 wild-type and *Ryk*-deficient cochleae. Bundle orientations are confined to a 45° segment centered on a line parallel to the medial-lateral axis in wild-type embryos. However, the distribution of OHC3 orientation is broader in the $Ryk^{-/-}$ mice. Stereociliary bundle orientation data were collected from three embryos of each genotype.

VANGL2 and that the RYK PDZ-binding motif is required at least in part for this interaction.

RYK may interact with VANGL2 in other PCP pathway signaling phenotypes, such as in zebrafish CE. To determine whether VANGL2 overexpression is able to rescue the Ryk MO-dependent reduction of embryo body length, zebrafish embryos were injected with Ryk MO-1 alone, human VANGL2 RNA alone, or Ryk MO-1 + VANGL2 RNA, and body length was quantified. Embryos injected with VANGL2 RNA alone showed a significant reduction in body length (Fig. 7*B*). Injection with Ryk MO-1 + VANGL2 RNA resulted in a significantly increased body length compared with embryos injected with RYK MO-1 alone (Fig. 7*B*), demonstrating that VANGL2 overexpression was partly able to rescue the RYK MO effects on zebrafish convergent extension.

Signaling downstream of PCP pathway activation is mediated by the small GTPases RhoA and Rac1 (1, 32). To determine whether RYK can activate RhoA, active RhoA (RhoA-GTP) pulldown assays were performed using GST-RBD in CHO-K1 cells. Cells transfected with full-length RYK had significantly higher active RhoA levels than empty vector-transfected cells (Fig. 7, *C* and *D*), which shows that RYK can activate RhoA. RYK activation of RhoA may be dependent on Wnt signaling. CHO-K1 cells transfected with Wnt3a showed activation of RhoA (~2-fold), which was inhibited in cells co-transfected with RYK siRNA (Fig. 7*E*), suggesting that Ryk is required for Wnt3a-induced RhoA activation in these cells. Overall, these results demonstrate that RYK protein interacts with PCP pathway proteins and activates Wnt/PCP downstream signaling.

DISCUSSION

Ryk is a member of the growth factor receptor family and plays a key role in a number of developmental processes in mammals, including craniofacial and skeletal development, axon guidance, axon extension, and neuronal differentiation (15–17). It has been identified as a receptor for the Wnt family of ligands, and previous studies have suggested a role for Ryk in both Wnt/β-catenin and β-catenin-independent Wnt signaling. Here, we show that Ryk acts to regulate classical Wnt/PCP pathway functions in mammals, as demonstrated in mouse inner ear development.

In this study, we analyzed the effect of Ryk function on the Wnt/β-catenin signaling pathway by using TCF-luciferase reporter assays. Previously, others have demonstrated that Ryk can activate Wnt/β-catenin signaling. TCF-luciferase reporter assays showed that Ryk was able to synergistically stimulate

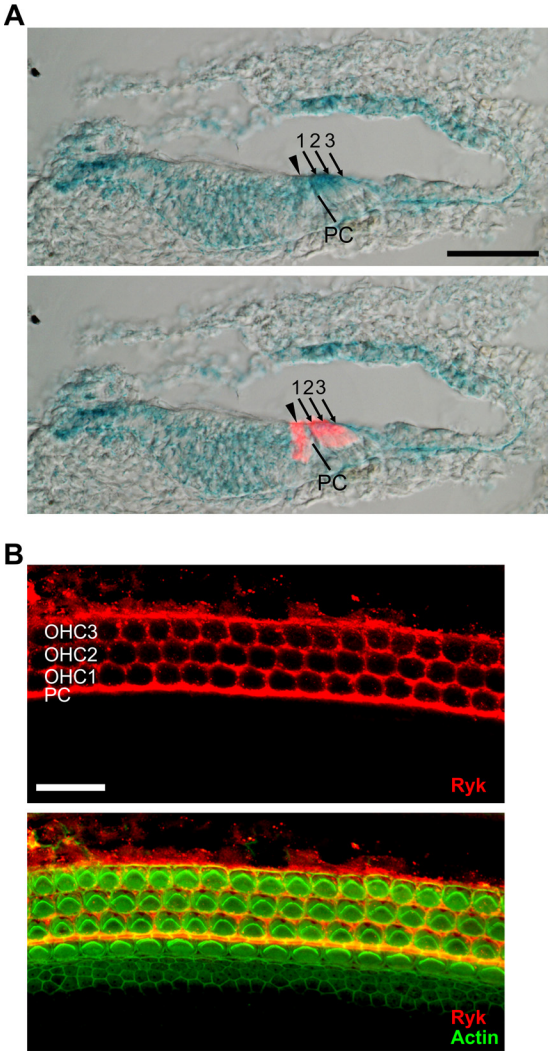

FIGURE 4. **Ryk is expressed in the mouse cochlea.** *A*, cross-section of an E18.5 Ryk-deficient ($Ryk^{LacZ/LacZ}$) cochlea showing β-gal staining (*blue*). *Ryk* mRNA was distributed throughout the cochlear duct, with strong expression in the OHCs and pillar cells (*PC*). In the *bottom panel*, the location of the hair cells is indicated with myosin 6 (*red*). A single IHC row (*arrowhead*) and three OHC rows (*arrows 1–3*) can be identified in the organ of Corti. *Scale bar,* 50 μm. *B*, surface view of a P0 wild-type mouse cochlear whole mount, showing Ryk protein expression in outer hair cells (*OHC1–3*) and pillar cells (*PC*) using an anti-Ryk antibody (*top panel*). The *bottom panel* shows co-staining with phalloidin (to detect actin). *Scale bar,* 20 μm.

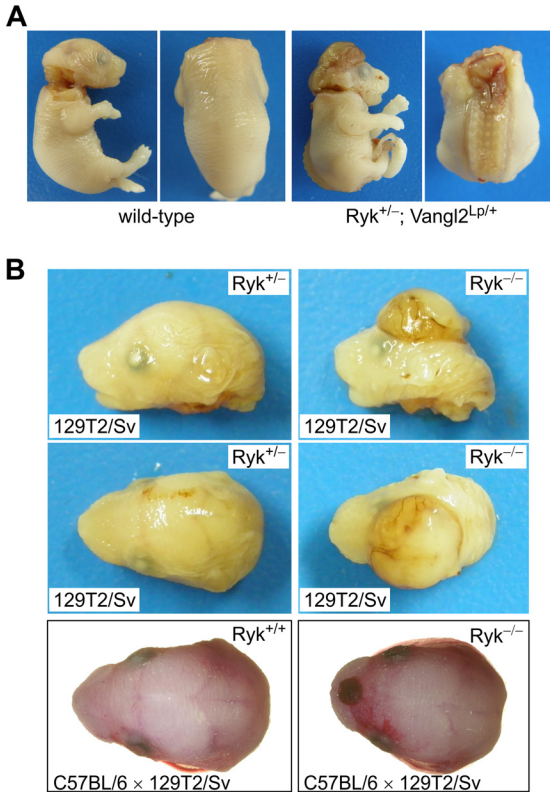

FIGURE 5. **Ryk-deficient mouse embryos display neural tube defects in specific genetic backgrounds.** *A*, lateral and dorsal views of a wild-type and a *Ryk* × *Vangl2* double-heterozygous ($Ryk^{+/-}$;$Vangl2^{Lp/+}$) E18.5 embryo from the same litter. The neural tube is open along its whole length in the double heterozygote. Embryo heads were removed in dorsal view images. *B*, $Ryk^{+/+}$/$Ryk^{+/-}$ and $Ryk^{-/-}$ E18.5 embryo heads from mice on a 129T2/Sv or a mixed C57BL/6 × 129T2/Sv genetic background; embryos sharing a genetic background were from the same litter. The 129T2/Sv knock-out has an open neural tube at the head only (exencephaly); this phenotype was observed in 13% of $Ryk^{-/-}$ embryos on this genetic background. No exencephaly was observed in $Ryk^{-/-}$ embryos on a mixed background.

luciferase activity when in the presence of Wnt3a (18). This study contradicts these data, as both full-length Ryk and soluble Ryk ECD constructs were unable to stimulate Wnt/β-catenin signaling. In contrast, a chimeric construct of WIF-1 containing the Ryk WIF domain was able to partially inhibit Wnt3a-stimulated signaling, although the inhibition was not as strong as observed for WIF-1 containing its endogenous WIF domain.

These contradictory results may be partly due to differences in the luciferase constructs used. The highly sensitive super-TOP-FLASH was used in this study, which, due to the presence of eight TCF sites in the promoter region (as opposed to three TCF sites in the TOP-FLASH vector that was used previously (18)), allows a greater range of Wnt3a activation to be observed. Our results are supported by a study that showed no further stimulation of TCF-luciferase reporter activity in HEK293T cells expressing full-length Ryk after Wnt3 treatment (33). Another possible explanation of the results is that HEK293T cells may have high endogenous levels of RYK protein, such that RYK overexpression would not further stimulate β-catenin activity. Support for this interpretation comes from a recent study showing that Ryk siRNAs could inhibit Wnt3a-stimulated β-catenin-activated reporter activity and Wnt/β-catenin target gene expression (34).

In the zebrafish embryo studies, Ryk MOs caused a reduction in body length and acted synergistically with a Wnt11 MO to further reduce body length and interocular distance. Phenotypes such as body length and interocular distance are determined by molecular pathways that control CE, including the Wnt/PCP pathway. Recently, it was shown that Wnt5b interacts with Ryk in zebrafish CE movements, potentially via the Wnt/calcium signaling pathway (24). Work by Kim *et al.* (14) in *X. laevis* has shown that Ryk MOs cause CE defects and that these can be rescued by RhoA overexpression. Moreover, they determined that Ryk MOs could rescue Wnt11 overexpression. Our zebrafish studies therefore agree with the previously published data demonstrating a role for Ryk in CE and its genetic interaction with Wnt11.

Misoriented stereociliary bundles in mouse mechanosensory hair cells strongly point to a PCP defect in $Ryk^{-/-}$ mice. We

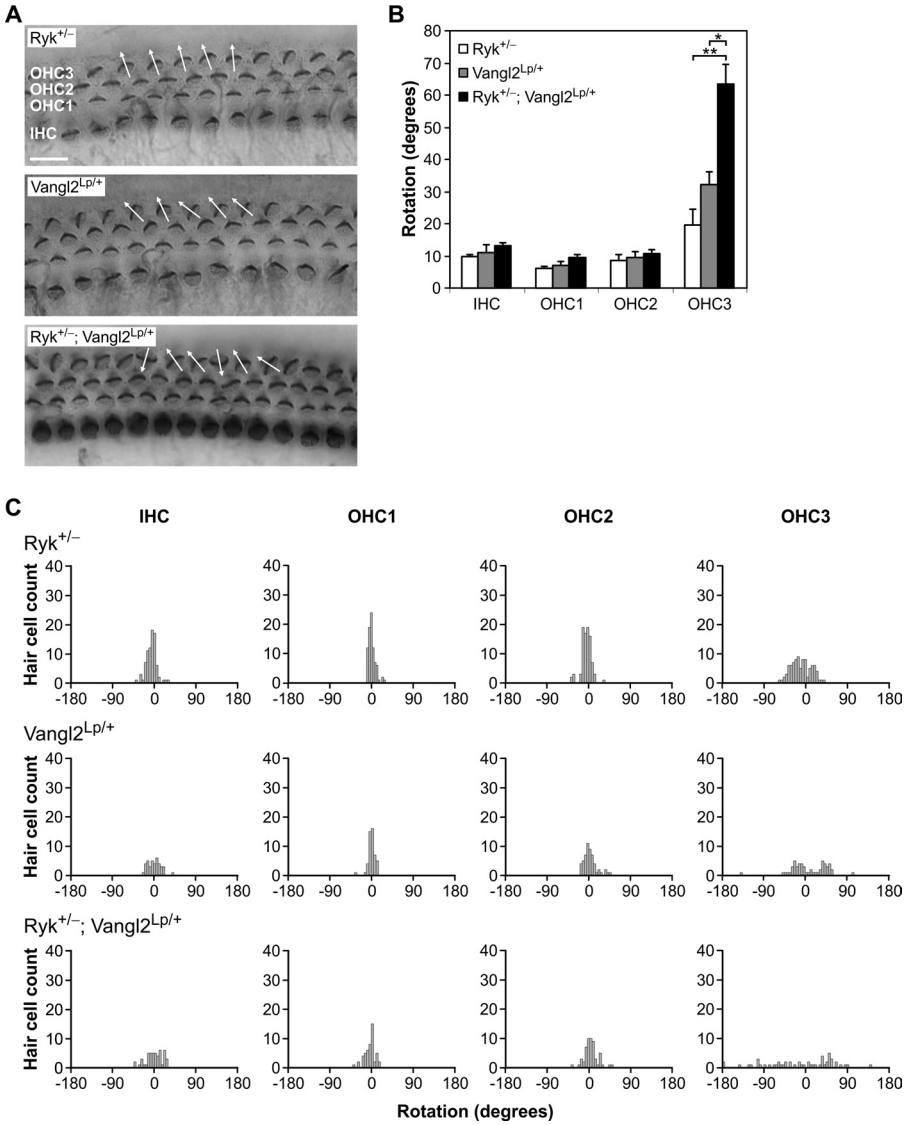

FIGURE 6. **Crosses of Ryk-deficient mice with Vangl2 mutant mice reveal that Ryk interacts with core PCP proteins in the cochlea.** *A*, cochleae from E18.5 embryos with genotypes *Ryk*$^{+/-}$, *Vangl2*$^{Lp/+}$, and double heterozygotes *Ryk*$^{+/-}$;*Vangl2*$^{Lp/+}$ were stained with *G. simplicifolia* lectin and examined at the mid-point of the sensory epithelia. *Arrows* show the orientation of some misoriented hair cells (*OHC3*). *Scale bar,* 10 μm. *B*, analysis of the orientation of hair cell stereociliary bundles. Results represent the mean ± S.E. for three embryos. *, $p < 0.05$; **, $p < 0.01$. *C*, comparison of distribution histograms for stereociliary bundle orientation in E18.5 mouse cochleae. Bundle orientations in *Ryk*$^{+/-}$ and *Vangl2*$^{Lp/+}$ cochleae are confined to a 60° segment centered on a line parallel to the medial-lateral axis. However, in the *Ryk*$^{+/-}$;*Vangl2*$^{Lp/+}$ double-heterozygous cochleae the distribution of OHC3 orientation is markedly broader. Stereociliary bundle orientation data were collected from three embryos of each genotype.

observed Ryk mRNA and protein expression in outer hair cells of late embryonic and neonatal mouse cochlea, confirming that the phenotype observed in *Ryk*$^{-/-}$ mice was due to a lack of Ryk expression. This misorientation phenotype has been linked to mutations in genes including *Celsr1*, the ortholog of the *Drosophila melanogaster* gene *flamingo*; *Vangl2*, the ortholog of *strabismus*/*van gogh*; and *Scrib1*, the *scribble* ortholog, which are all known to be PCP pathway genes in *D. melanogaster* (1, 8, 31). Other Wnt pathway protein mutants that have stereociliary bundle orientation defects include *Dvl1*, *Dvl2* double knock-outs, and *Fzd3*, *Fzd6* double knock-outs (35, 36).

Although exencephaly can be caused by perturbation of several processes, including disrupted sonic hedgehog signaling or ciliary gene mutations, it has also been observed in Wnt/PCP pathway mutants such as *Dvl3*$^{+/-}$;*Vangl2*$^{Lp/+}$ double heterozygotes (10, 37). This suggests that the Wnt/PCP pathway is involved in rostral neural tube closure and that the *Ryk*$^{-/-}$ mouse exencephaly phenotype may also be due to defects in PCP signaling.

Definitive proof of the genetic interaction between Ryk and PCP signaling comes from the phenotypes observed in the *Ryk*$^{+/-}$;*Vangl2*$^{Lp/+}$ double-heterozygous mice. *Looptail* is a naturally occurring mutation in the mouse *Vangl2* gene, which encodes for a four transmembrane domain protein. Vangl2 cooperates with the Wnt receptors Fzd or Ror2 to activate signaling via Dvl (38, 39) and the downstream RhoA/ROCK and Rac1 pathways (40, 41). The observations that mice with deletion of one Ryk allele combined with one *Vangl2*^{Lp} allele have severe neural tube defects and misoriented mechanosensory hair cells in the cochlea provide strong evidence of a role for Ryk in the mammalian PCP pathway.

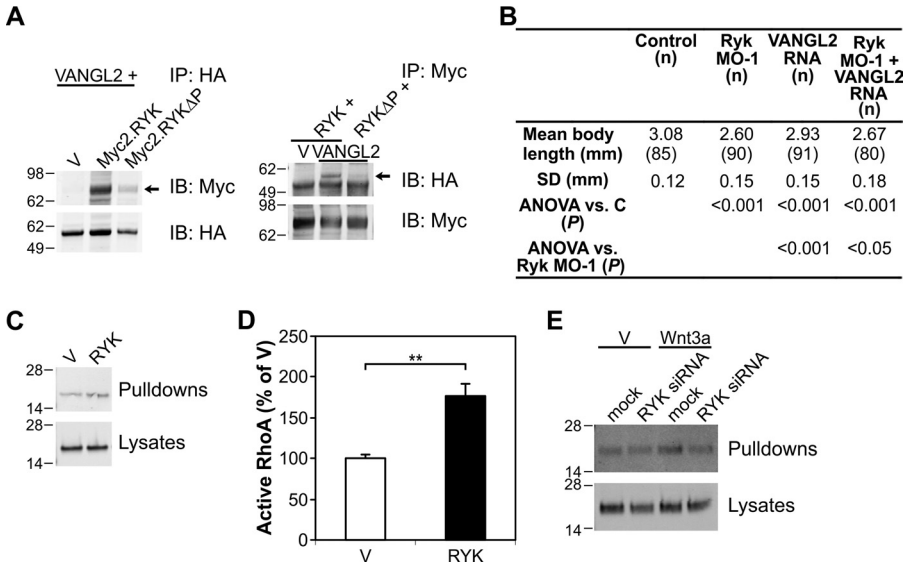

	Control (n)	Ryk MO-1 (n)	VANGL2 RNA (n)	Ryk MO-1 + VANGL2 RNA (n)
Mean body length (mm)	3.08 (85)	2.60 (90)	2.93 (91)	2.67 (80)
SD (mm)	0.12	0.15	0.15	0.18
ANOVA vs. C (*P*)		<0.001	<0.001	<0.001
ANOVA vs. Ryk MO-1 (*P*)			<0.001	<0.05

FIGURE 7. **RYK forms a complex with VANGL2 and activates RhoA.** *A*, immunoprecipitation (*IP*) of 200 μg of lysate from HEK293T cells transfected with empty vector (*V*), Myc2.RYK, Myc2.RYKΔPDZBM (*RYKΔP*), or HA2.VANGL2. *Arrows* indicate the band of interest (RYK constructs on the *left* or VANGL2 on the *right*). *B*, quantitation of body length in zebrafish embryos injected with Ryk MO-1 and VANGL2 RNA. (*n*), number of embryos analyzed in each treatment; *SD*, standard deviation of body length; *C*, control embryos; *ANOVA*, analysis of variance. *C*, active RhoA pulldowns using 1 ml of cell lysate from CHO-K1 cells transfected with empty vector (*V*) or RYKFCT. Western blot was performed with pulldowns or 10 μl of lysate using anti-RhoA antibody. *D*, quantitation of CHO-K1 cell lysate active RhoA pulldowns. Results represent the mean ± S.D. of three independent experiments. **, $p < 0.01$. *E*, active RhoA pulldowns using 1 ml of cell lysate from CHO-K1 cells mock transfected (no siRNA) or transfected with RYK siRNA and then transfected with empty vector (*V*) or Wnt3a.Myc5 (Wnt3a). Western blot was performed with pulldowns or 10 μl of lysate using anti-RhoA antibody. *IB*, immunoblot.

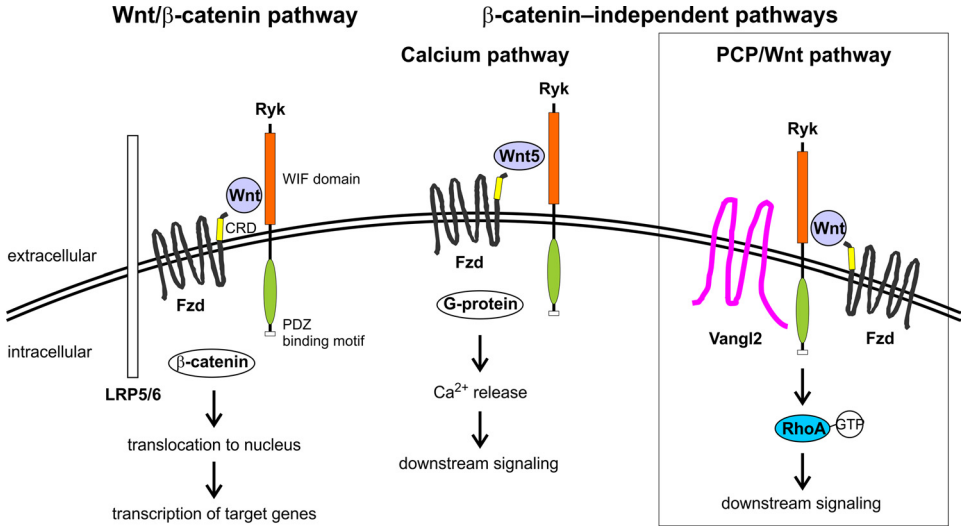

FIGURE 8. **Schematic diagram of the interaction between Ryk and Wnt signaling pathways.** Ryk binds to Wnts via its WIF domain and modulates both Wnt/β-catenin and β-catenin-independent signaling (14, 18, 22, 24). As was shown in this study, Ryk interacts with the PCP pathway protein Vangl2 and can activate downstream RhoA signaling (*boxed*). *CRD*, cysteine-rich domain; *Fzd*, Frizzled; *LRP5/6*, low density lipoprotein-related protein 5 or 6; *PDZ*, PSD-95/Dlg/ZO-1 homology; *WIF*, Wnt inhibitory factor.

The co-immunoprecipitation of RYK and VANGL2 proteins in this study further supports a role for Ryk in PCP signaling. It is likely that the RYK PDZ-binding motif, located at the extreme carboxyl terminus of the protein, is required for interaction with VANGL2. In addition, the finding that VANGL2 overexpression in zebrafish embryos was able to partly rescue the Ryk MO-1 effects on body length strengthens the role of the *in vivo* interaction between RYK and VANGL2. The finding that there was only partial rescue of the Ryk MO phenotype suggests that Ryk regulation of CE may be mediated via other signaling proteins. However, it is also possible that human *VANGL2* mRNA was not as effective at rescuing Ryk MO effects as the zebrafish *Vangl2* mRNA would have been, as was observed previously for *Vangl1* mRNA (42).

It was previously shown that treatment of CHO-K1 cells with Wnt3a results in RhoA activation (43). Our findings that RYK overexpression increases active RhoA levels in CHO-K1 cells and that Wnt3a-stimulated RhoA activation requires endogenous Ryk expression provide a downstream pathway by which RYK may activate Wnt/PCP signaling (Fig. 8).

Other phenotypes associated with the Ryk-deficient mice, such as skeletal and craniofacial defects, may also have their origins in disruption of Wnt signaling via the Ryk receptor. The complexity of these phenotypes means that it may take some

time to unravel their link to the Wnt/β-catenin or β-catenin-independent pathways. It was recently shown that RYK protein can pull down both Wnt/β-catenin and PCP pathway proteins in HEK293T cells, including β-catenin itself, as well as CELSR1, CELSR2, and CELSR3 (34). Alternatively, there may be other ligands for Ryk that provide distinct or Wnt-independent signal transduction responsible for these phenotypes. Ryk has been shown to interact biochemically with the receptor tyrosine kinases EphB2 and EphB3 and the cell scaffold protein AF-6 (afadin) (15, 44). These proteins may be components of the Ryk-Vangl2 protein complex and therefore may be important for Ryk function in Wnt/PCP signaling.

Taken together, the results of this study strongly support a role for Ryk in PCP signaling via Vangl2. The specific Wnts required for Ryk signaling are still unknown, although the synergistic *in vivo* effects in zebrafish experiments suggest that Wnt11 may interact with Ryk in this signaling pathway. Future studies will further characterize Ryk-interacting proteins, thus contributing to our knowledge of the PCP pathway in vertebrate development.

Acknowledgments—We thank R. Moon for the superTOP-FLASH and superFOP-FLASH plasmids; A. McMahon for the Wnt3a and Wnt11 plasmids; R. Habas for the pGEX-RBD plasmid; Y. Zou for the anti-Ryk antibodies; S. Jane for providing the Vangl2^{Lp} mice; A. Naughton and staff at the Biological Resource Facility at the Ludwig Institute for Cancer Research, Melbourne, Australia, for assistance with mouse experiments; S. Cody for assistance with imaging; S. Paquet-Fifield for assistance with photography; and M. Achen for critical reading of the manuscript. Fluorescent images were generated at the University of California, San Diego, Neuroscience Microscopy Shared Facility supported by National Institutes of Health NS/NINDS HHS Grant P30-NS047101.

REFERENCES

1. Seifert, J. R., and Mlodzik, M. (2007) Frizzled/PCP signaling. A conserved mechanism regulating cell polarity and directed motility. *Nat. Rev. Genet.* **8,** 126–138
2. Keller, R. (2002) Shaping the vertebrate body plan by polarized embryonic cell movements. *Science* **298,** 1950–1954
3. Tada, M., and Smith, J. C. (2000) Xwnt11 is a target of *Xenopus* Brachyury; Regulation of gastrulation movements via Dishevelled but not through the canonical Wnt pathway. *Development* **127,** 2227–2238
4. Wallingford, J. B., Rowning, B. A., Vogeli, K. M., Rothbächer, U., Fraser, S. E., and Harland, R. M. (2000) Dishevelled controls cell polarity during *Xenopus* gastrulation. *Nature* **405,** 81–85
5. Heisenberg, C. P., Tada, M., Rauch, G. J., Saúde, L., Concha, M. L., Geisler, R., Stemple, D. L., Smith, J. C., and Wilson, S. W. (2000) Silberblick/Wnt11 mediates convergent extension movements during zebrafish gastrulation. *Nature* **405,** 76–81
6. Strong, L. C., and Hollander, W. F. (1949) Hereditary loop-tail in the house mouse. Accompanied by imperforate vagina and with lethal craniorachischisis when homozygous. *J. Heredity* **40,** 329–334
7. Stein, K. F., and Rudin, I. A. (1953) Development of mice homozygous for the gene for looptail. *J. Heredity* **44,** 59–69
8. Montcouquiol, M., Rachel, R. A., Lanford, P. J., Copeland, N. G., Jenkins, N. A., and Kelley, M. W. (2003) Identification of *Vangl2* and *Scrb1* as planar polarity genes in mammals. *Nature* **423,** 173–177
9. Qian, D., Jones, C., Rzadzinska, A., Mark, S., Zhang, X., Steel, K. P., Dai, X., and Chen, P. (2007) Wnt5a functions in planar cell polarity regulation in mice. *Dev. Biol.* **306,** 121–133
10. Etheridge, S. L., Ray, S., Li, S., Hamblet, N. S., Lijam, N., Tsang, M., Greer, J., Kardos, N., Wang, J., Sussman, D. J., Chen, P., and Wynshaw-Boris, A. (2008) Murine Dishevelled 3 functions in redundant pathways with Dishevelled 1 and 2 in normal cardiac outflow tract, cochlea, and neural tube development. *PLoS Genet.* **4,** e1000259
11. Hovens, C. M., Stacker, S. A., Andres, A. C., Harpur, A. G., Ziemiecki, A., and Wilks, A. F. (1992) RYK, a receptor tyrosine kinase-related molecule with unusual kinase domain motifs. *Proc. Natl. Acad. Sci. U.S.A.* **89,** 11818–11822
12. Stacker, S. A., Hovens, C. M., Vitali, A., Pritchard, M. A., Baker, E., Sutherland, G. R., and Wilks, A. F. (1993) Molecular cloning and chromosomal localization of the human homologue of a receptor related to tyrosine kinases (RYK). *Oncogene* **8,** 1347–1356
13. Macheda, M. L., and Stacker, S. A. (2008) Importance of Wnt signaling in the tumor stroma microenvironment. *Curr. Cancer Drug Targets* **8,** 454–465
14. Kim, G. H., Her, J. H., and Han, J. K. (2008) Ryk cooperates with Frizzled 7 to promote Wnt11-mediated endocytosis and is essential for *Xenopus laevis* convergent extension movements. *J. Cell Biol.* **182,** 1073–1082
15. Halford, M. M., Armes, J., Buchert, M., Meskenaite, V., Grail, D., Hibbs, M. L., Wilks, A. F., Farlie, P. G., Newgreen, D. F., Hovens, C. M., and Stacker, S. A. (2000) Ryk-deficient mice exhibit craniofacial defects associated with perturbed Eph receptor cross-talk. *Nat. Genet.* **25,** 414–418
16. Keeble, T. R., Halford, M. M., Seaman, C., Kee, N., Macheda, M., Anderson, R. B., Stacker, S. A., and Cooper, H. M. (2006) The Wnt receptor Ryk is required for Wnt5a-mediated axon guidance on the contralateral side of the corpus callosum. *J. Neurosci.* **26,** 5840–5848
17. Zhong, J., Kim, H. T., Lyu, J., Yoshikawa, K., Nakafuku, M., and Lu, W. (2011) The Wnt receptor Ryk controls specification of GABAergic neurons *versus* oligodendrocytes during telencephalon development. *Development* **138,** 409–419
18. Lu, W., Yamamoto, V., Ortega, B., and Baltimore, D. (2004) Mammalian Ryk is a Wnt coreceptor required for stimulation of neurite outgrowth. *Cell* **119,** 97–108
19. Liu, Y., Shi, J., Lu, C. C., Wang, Z. B., Lyuksyutova, A. I., Song, X. J., Song, X., and Zou, Y. (2005) Ryk-mediated Wnt repulsion regulates posterior-directed growth of corticospinal tract. *Nat. Neurosci.* **8,** 1151–1159
20. Schmitt, A. M., Shi, J., Wolf, A. M., Lu, C. C., King, L. A., and Zou, Y. (2006) Wnt-Ryk signaling mediates medial-lateral retinotectal topographic mapping. *Nature* **439,** 31–37
21. Halford, M. M., and Stacker, S. A. (2001) Revelations of the RYK receptor. *BioEssays* **23,** 34–45
22. Li, L., Hutchins, B. I., and Kalil, K. (2009) Wnt5a induces simultaneous cortical axon outgrowth and repulsive axon guidance through distinct signaling mechanisms. *J. Neurosci.* **29,** 5873–5883
23. Blakely, B. D., Bye, C. R., Fernando, C. V., Horne, M. K., Macheda, M. L., Stacker, S. A., Arenas, E., and Parish, C. L. (2011) Wnt5a regulates midbrain dopaminergic axon growth and guidance. *PLoS One* **6,** e18373
24. Lin, S., Baye, L. M., Westfall, T. A., and Slusarski, D. C. (2010) Wnt5b-Ryk pathway provides directional signals to regulate gastrulation movement. *J. Cell Biol.* **190,** 263–278
25. Stacker, S. A., Stenvers, K., Caesar, C., Vitali, A., Domagala, T., Nice, E., Roufail, S., Simpson, R. J., Moritz, R., Karpanen, T., Alitalo, K., and Achen, M. G. (1999) Biosynthesis of vascular endothelial growth factor-D involves proteolytic processing that generates noncovalent homodimers. *J. Biol. Chem.* **274,** 32127–32136
26. Lele, Z., Bakkers, J., and Hammerschmidt, M. (2001) Morpholino phenocopies of the *swirl*, *snailhouse*, *somitabun*, *minifin*, *silberblick*, and *pipetail* mutations. *Genesis* **30,** 190–194
27. Dabdoub, A., Donohue, M. J., Brennan, A., Wolf, V., Montcouquiol, M., Sassoon, D. A., Hseih, J. C., Rubin, J. S., Salinas, P. C., and Kelley, M. W. (2003) Wnt signaling mediates reorientation of outer hair cell stereociliary bundles in the mammalian cochlea. *Development* **130,** 2375–2384
28. Dabdoub, A., Puligilla, C., Jones, J. M., Fritzsch, B., Cheah, K. S., Pevny, L. H., and Kelley, M. W. (2008) Sox2 signaling in prosensory domain specification and subsequent hair cell differentiation in the developing cochlea. *Proc. Natl. Acad. Sci. U.S.A.* **105,** 18396–18401
29. Heisenberg, C. P., and Nüsslein-Volhard, C. (1997) The function of *silberblick* in the positioning of the eye anlage in the zebrafish embryo. *Dev. Biol.*

184, 85–94
30. Jopling, C., and den Hertog, J. (2005) Fyn/Yes and noncanonical Wnt signaling converge on RhoA in vertebrate gastrulation cell movements. *EMBO Rep.* **6,** 426–431
31. Curtin, J. A., Quint, E., Tsipouri, V., Arkell, R. M., Cattanach, B., Copp, A. J., Henderson, D. J., Spurr, N., Stanier, P., Fisher, E. M., Nolan, P. M., Steel, K. P., Brown, S. D., Gray, I. C., and Murdoch, J. N. (2003) Mutation of *Celsr1* disrupts planar polarity of inner ear hair cells and causes severe neural tube defects in the mouse. *Curr. Biol.* **13,** 1129–1133
32. Habas, R., Dawid, I. B., and He, X. (2003) Coactivation of Rac and Rho by Wnt/Frizzled signaling is required for vertebrate gastrulation. *Genes Dev.* **17,** 295–309
33. Lyu, J., Yamamoto, V., and Lu, W. (2008) Cleavage of the Wnt receptor Ryk regulates neuronal differentiation during cortical neurogenesis. *Dev. Cell* **15,** 773–780
34. Berndt, J. D., Aoyagi, A., Yang, P., Anastas, J. N., Tang, L., and Moon, R. T. (2011) Mindbomb 1, an E3 ubiquitin ligase, forms a complex with RYK to activate Wnt/β-catenin signaling. *J. Cell Biol.* **194,** 737–750
35. Wang, J., Mark, S., Zhang, X., Qian, D., Yoo, S. J., Radde-Gallwitz, K., Zhang, Y., Lin, X., Collazo, A., Wynshaw-Boris, A., and Chen, P. (2005) Regulation of polarized extension and planar cell polarity in the cochlea by the vertebrate PCP pathway. *Nat. Genet.* **37,** 980–985
36. Wang, Y., Guo, N., and Nathans, J. (2006) The role of *Frizzled3* and *Frizzled6* in neural tube closure and in the planar polarity of inner-ear sensory hair cells. *J. Neurosci.* **26,** 2147–2156
37. Wu, G., Huang, X., Hua, Y., and Mu, D. (2011) Roles of planar cell polarity pathways in the development of neutral tube defects. *J. Biomed. Sci.* **18,** 66
38. Gao, B., Song, H., Bishop, K., Elliot, G., Garrett, L., English, M. A., Andre, P., Robinson, J., Sood, R., Minami, Y., Economides, A. N., and Yang, Y. (2011) Wnt signaling gradients establish planar cell polarity by inducing Vangl2 phosphorylation through Ror2. *Dev. Cell* **20,** 163–176
39. Shafer, B., Onishi, K., Lo, C., Colakoglu, G., and Zou, Y. (2011) Vangl2 promotes Wnt/planar cell polarity-like signaling by antagonizing Dvl1-mediated feedback inhibition in growth cone guidance. *Dev. Cell* **20,** 177–191
40. Ybot-Gonzalez, P., Savery, D., Gerrelli, D., Signore, M., Mitchell, C. E., Faux, C. H., Greene, N. D., and Copp, A. J. (2007) Convergent extension, planar-cell-polarity signaling and initiation of mouse neural tube closure. *Development* **134,** 789–799
41. Lindqvist, M., Horn, Z., Bryja, V., Schulte, G., Papachristou, P., Ajima, R., Dyberg, C., Arenas, E., Yamaguchi, T. P., Lagercrantz, H., and Ringstedt, T. (2010) Vang-like protein 2 and Rac1 interact to regulate adherens junctions. *J. Cell Sci.* **123,** 472–483
42. Reynolds, A., McDearmid, J. R., Lachance, S., De Marco, P., Merello, E., Capra, V., Gros, P., Drapeau, P., and Kibar, Z. (2010) VANGL1 rare variants associated with neural tube defects affect convergent extension in zebrafish. *Mech. Dev.* **127,** 385–392
43. Endo, Y., Wolf, V., Muraiso, K., Kamijo, K., Soon, L., Uren, A., Barshishat-Küpper, M., and Rubin, J. S. (2005) Wnt-3a-dependent cell motility involves RhoA activation and is specifically regulated by Dishevelled-2. *J. Biol. Chem.* **280,** 777–786
44. Kamitori, K., Tanaka, M., Okuno-Hirasawa, T., and Kohsaka, S. (2005) Receptor related to tyrosine kinase RYK regulates cell migration during cortical development. *Biochem. Biophys. Res. Commun.* **330,** 446–453